Quantifying the contributing factors towards signal fatigue in nanocomposite strain sensors

Article (Accepted Version)

Quantifying the Contributing Factors towards Signal Fatigue in Nanocomposite Strain Sensors

Conor S Boland*

School of Mathematical and Physical Sciences, University of Sussex, Brighton, BN1 9QH, United Kingdom

*c.s.boland@sussex.ac.uk

Keywords: nanocomposite, strain sensor, electromechanics, Mullin's effect, fatigue, Basquin's law, model, bodily sensor

Abstract

With unparalleled sensitivities, nanocomposites are believed to be key components in future bodily sensor and healthcare devices. However, there is a lack in understanding of how repeated strain cycles effect their electromechanical performance and what measures can be taken to accommodate changes in measurement using modelling and signal processing. Here, the author examines published cyclic data from a wide range of nanocomposite strain sensors. From the datasets, the author reports a near universal scaling in electromechanical signal with cycle number (C) as a result of the Mullin's effect. Using a modified model based on Basquin's law of fatigue, for all nanocomposites, signal was found to following a nearly identical $C^{-0.1}$ power law scaling with cycle number. Using the presented model, the author demonstrated that a critical conditioning cycle number for a nanocomposite at which a steady state signal occurs, known as the endurance limit, can be predicted. Endurance limit was reported to be highly dependent on the scaling exponent noted in the cyclic data.

Introduction

Research into the electromechanical properties of elastomer-based composites filled with conductive nanomaterials are heralded as one of the great hopes of nanoscience reaching the consumer market place.[1, 2] Not just limited to one singular polymer or nanofiller type, these nanocomposite materials applied as strain sensors are paving the way towards the practical use of nanotechnologies outside of a laboratory setting.[2] From bodily movement to real-time vital signs measurement, nanocomposite sensors have far surpassed the performances of current commercial devices, being on average six times more sensitive.[3] These advances in research and their processability are quickly leading to the realisation of these materials even facilitating future robotic technologies.[4] In order to enable these lofty yet very realistic aspirations, nanocomposite strain sensors must display a large sustainable electromechanical response over a wide working range (*i.e.* large working factor).[3] Ideally, these sensing materials will have a signal that changes linearly with strain to accommodate performance metric extrapolation and signal processing. This linearity was reported to be highly dependent on the yield strain of a nanocomposite and the level aggregation present in the conductive filler network, with higher levels of aggregation decreasing signal linearity.[3]

However, the effect repeated or cyclic loading has on the electromechanical response of nanocomposites is widely unquantified and in many cases goes unreported.[3, 5] For their use in future technologies, nanocomposites must present a signal that is for the most part invariant and in literature this is generally examined through cyclic testing in which a material is repeatedly strained through a constant strain range with the electromechanical response simultaneously measured. Under cyclic loading conditions, two mechanisms can occur that lead to electromechanical response to either increase or decrease. The first mechanism is quite straightforward, in that, as cycle number increases the electromechanical response will also increase in magnitude or undergo a positive drift due to crack initiation, transverse microcracking, and delamination caused by plastic deformation in the polymer matrix.[6, 7] Ultimately this internalised cracking will result in the conductive filler network being artificially more sensitive to strain, resulting in the observed increase in electromechanical response with cycle number. [8-13] It is reported in CNT fibre nanocomposites that this change in composite

resistance will increase linearly with cycle number and could allow for such materials to be applied as damage sensors.[14] However, for health applications and using pulse measurement as an example, the average human heart will beat ~108,000 times a day and if a nanocomposite sensor begins to fail at ~1000s of cycles, it is simply not fit for purpose as a bodily sensor. Signal processing would unfortunately not be able to correct for the randomness in electromechanical response due to damage before failure and thus their usage lifetime would be far too short for such health monitoring applications.

For the second mechanism, there is a large observed electromechanical response during the first cycle, after which there is a decay in the magnitude of the signal with ensuing cycles.[5, 15, 16] Essentially, as a nanocomposite is being cycled there is an inadvertent decrease in sensitivity.[16, 17] However, it is believed that with conditioning cycles, where by a nanocomposite is subjected to a large number of cycles (~ 200 cycles), that this decay in signal will subside.[18-22] Nonetheless, in many cases in literature, there are examples of this decay still occurring even at >> 500 cycles.[23-29] Despite wide spread observation of sensitivity decay, some reports still only cycle materials for as little as ≤ 10 cycles and record no saturation point.[30, 31] The mechanism that controls this sensitivity decay to date has gone largely unexplored despite its implications on the future applications of these materials as components in bodily monitoring devices. In contrast to the first mechanism, if there were a model that could describe the decay in electromechanical response observed during cyclic loading or project a critical conditioning cycle number at which a steady state signal could be achieved, it would be a powerful predictive tool for the sensor research community. Through this model, signal processing could be used to correct for variations in electromechanical response thus facilitating future studies and applications.

Here, the author believes that through a detailed analysis of literary data a more complete view of how cyclic loading impacts electromechanical response of nanocomposites can be created. Through these data sets, an apparent power law dependence in signal with cycle number was observed; with this power law scaling found to be similar in all cases. It was found that this decrease in electromechanical signal was a direct consequence of the Mullin's effect, which describes a stress softening in elastomer composites with mechanical cycling. This implies that there is a direct link between mechanical

hysteresis and electromechanical response. Through this, a model based on Basquin's law of fatigue was created, where good agreement between data and theory was observed. Classically, from Basquin's law, a saturation point in stress softening is predicted and through the author's modified Basquinian model, an expression that projects the required number of conditioning cycles to reach a steady state in electromechanical response presented. The predicted values from this model were also found to match closely that of reported ones.

Results and Discussion

Trends in Literature Data

In order to assess the performance of nanocomposites during loading cycles, a detailed literature analysis was performed in which reports that presented data sets displaying electromechanical response as a function of loading cycles were used. This information comprised of data sets from nanocomposites with a vast array of morphologies and which applied an even larger variety of nanomaterials. Data was extrapolated accordingly from these sources (see Methods) and then plotted as a function of one another in Fig 1A. From this plot, it was noted that all data sets appear to follow similar power law scaling in fractional resistance change range $(\Delta R/R_0)_R$ (*i.e.* the height of the reported electromechanical signal) with cycle number (C). Power law scaling of $(\Delta R/R_0)_R \propto C^{-0.1}$ was denoted by dashed lines in the plot. When examining the literary data, in some cases, this scaling eventually reached a saturation point however, in many cases the decay seemed continuous. This scaling would seem to confirm that under cyclic loading conditions, a nanocomposite's electromechanical response will diminish as cycle number increases. In Fig 1B, a master plot of the normalised fractional resistance change range, $(\Delta R/R_0)_{R,norm}$, as a function of cycle number confirmed this apparent shared universal scaling in the electromechanical properties of nanocomposites as all sampled data sets appear to overlay one another closely. It is reported here that this scaling follows a near $C^{-0.1}$ dependency.

The Mullin's Effect in Nanocomposite Strain Sensors

For the materials described in the previous section, in all cases, they underwent tensile cyclic loads and thus experienced stresses occurring in the tensile realm. Under such conditions, materials can undergo

fatigue and as the material "tires" it can be begin to fail.[32] This failure can even occur at stresses and strains below the materials yield point.[32] More specifically, for elastomers filled with nanomaterials, they can undergo mechanisms involving chain breakage, void formation and filler microstructural degradation during cycling.[33]These mechanisms manifest themselves in nanocomposites as a loss of stiffness or softening of the material with increasing cycle number resulting in a decrease in stress range which is reflected as a downward shifting in hysteresis curves.[34] As noted previously, the largest decrease in resistance occurred when going from the first to second cycle,[31, 35] this in fact mirrors a maxima in stiffness and stress loss which is reported to take place during the first cycles of fatigue testing.[33] The decreasing in $(\Delta R/R_0)_R$ and stress with cycle number in some way must be connected.

The reported softening that occurs during cycling is known as the Mullin's effect.[36] Similar to the Payne effect, the Mullin's effect is the result of the structural evolution of glassy and soft microstructures inside a polymer/filler system as a function of repetitious strains.[34, 36] Softening can be attributed to a stress relaxation mechanism[34] that in the past was modelled by Kraus as the number of connections in a filler network inside a housing polymer matrix as function of strain amplitude.[36, 37] However, it has been noted that this softening is not permanent and stiffness maybe be partially recovered in nanocomposites as crystalline regions are reported to 'rebirth' ambiently over a long time scale (~10^6 s) at a rate that is temperature dependent.[38, 39]

Fillers inside polymer elastomer systems can be said to be surround or covered by crystalline polymer described as a 'glassy layer' and form interconnected networks containing 'glassy bridges' (red region) that adjoin neighbouring fillers (grey rectangles) inside the bulk amorphous structure (Fig 2A).[36, 38, 40-42] According to percolation theory, at a critical loading level of fillers, this network will enable the conduction of electrical current.[43-45] During loading for a elastomeric-based nanocomposite, fluidisation of the glassy layers and bridges occur (Fig 2B), resulting in a change in filler network structure impacting subsequent response to additional loading cycles (Fig 2C).[39] This fluidisation is caused by local heating from internalised friction in and around the glassy filler network as a result of bulk sliding of polymer chains by one another and chains sliding off of or on filler interfaces.[34, 39, 41, 42] In contrast, for brittle epoxy-based nanocomposites, cycling also leads to softening however hysteresis effects are

due to the propagation of voids and an increase in crack density.[46] For these materials, $(\Delta R/R_0)_R$ is found to increase with cycle number as opposed to decrease due to complete material failure.[47]

Quantifying Fatigue

When examining the fatigue experienced by a material brought about by the Mullin's effect, decay in mechanical stress amplitude in relation to repeated, constant low strain cycling can be plotted as a log-log graph, known as Wöhler's plot.[48] This scaling in stress amplitude can then be universally modelled using Basquin's law[48-51], rewritten below in terms of stress range (*i.e.* height of stress signal)

$$\sigma_R = \sigma_0 C^{-B} \quad \text{(Eq. 1)}$$

Essentially, this expression describes a power law decay in the measured stress range (σ_R) with cycle number (C) up until a saturation point, known as the endurance limit (C_E), at which the stress decay slope becomes infinitesimally small and the failure limit is said to be infinite.[48, 51] Here, σ_0 is a material constant related to the stress range after one cycle and B is the Basquin exponent which is a universal constant equal to ~0.1[48, 51] but has been reported to vary between ~0.05 and ~0.2 depending on material properties.[49] It is important to note that Basquin's law can only be applied to cycling conditions below the yield point.[52] In Fig 3A-B, we have hypothetical cyclic mechanical data displaying the characteristics of the Mullin's effect. From extrapolating σ_R from Fig. 3B, a Wöhler's plot can be produced in Fig. 3C. From this plot, Basquin-liking scaling was observed and through fitting Eq. 1, this assumption is confirmed by the $\sigma_R \propto C^{-0.1}$ scaling.

We can assume that for nanocomposites, though generally based on non-linear elastomer materials, if the deformation applied during cycling is small with respective to the yield point they should undergo Hookean-like linear elastic deformation.[33, 53] Through this, stress (σ) is related to the applied strain (ε) and the Young's modulus (E) by

$$\sigma = E\varepsilon \quad \text{(Eq. 2)}$$

So for a Hookean material, the stress range after one cycle can also be said to be

$$\sigma_R \approx E_0\varepsilon \quad \text{(Eq. 3)}$$

Where E_0 is the Young's modulus after one cycle. Thus, we can relate this expression to Eq. 1 and rewrite it as

$$E_0\varepsilon \approx \sigma_0 C^{-B} \quad \text{(Eq. 4)}$$

For electrically conductive nanocomposite materials, their fractional electrical resistance range will linearly change with applied strain up until the yield point according to the following[3]

$$\left(\frac{\Delta R}{R_0}\right)_{R,1} = G_0\varepsilon \quad \text{(Eq. 5)}$$

Where $(\Delta R/R_0)_{R,1}$ and G_0 are the fractional resistance change range and the sensitive metric, the gauge factor, after one cycle respectively. Taking Eq. 5, we can rearrange it in terms of strain and apply it to Eq. 4 to create an expression describing a power law decay in fractional resistance range with cycle number

$$\left(\frac{\Delta R}{R_0}\right)_{R,C} \approx \frac{G_0\sigma_0}{E_0} C^{-B} \quad \text{(Eq. 6)}$$

We can then simply this expression as

$$\left(\frac{\Delta R}{R_0}\right)_{R,C} \approx \alpha C^{-B} \quad \text{(Eq. 7)}$$

Similar to what was overserved in literary data sets in Fig 1., this relationship implies that as a nanocomposite undergoes a cycling regime, in theory, signal range and thus sensitivity will scale as $C^{-0.1}$.

Apparent Universal Fatigue Scaling in Electromechanical Response

In accordance with Basquin's law, it is predicted that the fractional resistance change range of a nanocomposites during cycling will scale as C^{-B}, where the exponent should be near ~0.1. To confirm this, all data sets (see SI Fig. S1-S7) were fitted to extrapolate the Basquin exponent (see SI Table S1), with the values of exponent plotted as a function of the maximum cycle number (C_{max}) in Fig 4. From this plot it was seen that values for B are found to vary between 0.02 and 0.4 and in comparison to other nanocomposite systems like epoxies[52, 54] and thermoplastics,[55, 56] these values are within the expected

range. It was found though that the majority of datasets however lay in and around the predicted theoretical value of 0.1 (denoted by the dashed red line), with the mean value for the Basquin exponent from 54 datasets calculated to be 0.108 ± 0.011. In accordance with theory,[57] it was also observed that there were several examples of the scaling exponent to be rate and frequency independent (see SI Table S1).[27, 58-60] Furthermore, the validity of the model was reaffirmed in SI Fig. S8, where theoretical values for α, extrapolated through fitting Eq.7 to SI Fig S1-S7, were plotted against experimentally calculated values using the description of α from Eq. 6 and the corresponding literary data in SI Table S2. Both theory and experimental values were found to be in good agreement. Thus, the presence of the observed scaling in the electromechanical response of nanocomposites with cycle number was confirmed to be a manifestation of the Mullin's effect on stress amplitude during cycling that presents scaling predicted by Basquin's law.

Endurance Limit of Electromechanical Signal

As previously stated, the response in electromechanical signal is expected to follow a similar trend predicted by fatigue theory. According to this theory, at an endurance limit, the scaling in stress softening will cease. At this limit, σ_R reaches its minimum steady state value of $\sigma_{R,min}$ where all deformation within the material will be elastic.[61] In general, at this limit, the ratio between $\sigma_{R,min}$ and σ_0, known as the fatigue ratio,[61] can be approximated to 0.5[61, 62] for elastomers. For our nanocomposite materials here, this can be expressed as

$$\left(\frac{\Delta R}{R_0}\right)_{R,min} \approx 0.5\alpha \quad \text{(Eq. 8)}$$

Using this expression, we can rewrite Eq. 7 in terms of the endurance limit, C_E

$$0.5\alpha \approx \alpha C_E^{-B} \quad \text{(Eq. 9)}$$

Simplifying and rearranging this gets

$$\ln(C_E) \approx \frac{\ln(0.5)}{-B} \quad \text{(Eq. 10)}$$

Now, simplifying Eq. 10 we arrive at a relationship between C_E and B that predicts a theoretical value for the number of cycles required to condition a nanocomposite to achieve a steady state in signal.

$$C_E \approx e^{\frac{\ln(0.5)}{-B}} \quad \text{(Eq. 11)}$$

Using Eq. 11 and values for Basquin's exponent from Fig. 4, calculated values of C_E were plotted as a function of B in Fig. 5. From this plot, for values of $B \geq 0.1$ (dashed red line), its reported that the number of conditioning cycles required to reach a steady state can be said to be at a minimum. The cycles requirement in this region presents values of $C_E \leq 1000$ (dashed blue line) and can be interpreted as a region of optimum processability. Below these values for B (*i.e.*≤ 0.1), the number of conditioning cycles required to reach C_E dramatically increases. Looking at experimental values of C_E reported in literature or observed from plotting SI Fig. S1-S7 (see SI Table S3) plotted against values predicted by Eq. 11 (see SI Table S1) in Fig S9 are once again observed to be in close agreement.

Retrospective Impact

From the model presented, we can now understand on a fundamental level not only what causes conditioning in nanocomposite strain sensors but also why some materials, though not presenting any obvious signs of materials degradation, never report a steady signal. However, it can also be said that there are several examples of nanocomposites reporting little to no discernible tread in $(\Delta R/R_0)_{R,C}$ with C. From this work, this can also now be attributed to their superior mechanical hysteresis as a result of fibre formation,[63-66] use of lament layers[63-66] and micro-structuring[67-70] which appears to quench effects of stress softening on electromechanical response. However, these morphologies, in particular the fibres, generally have larger values for Young's modulus which has been noted by the author in prior work as being a vital parameter of nanocomposites that must be minimised to facilitate applications as bodily sensors.[3] None the less, through the presented model here, the response signals in these engineered nanocomposite systems can now be viewed as possibly being a result of Basquin's exponent values being $B >> 0.1$. Thus leading to conditioning occurring over the first few strain cycles as predicted by Eq. 11.

Conclusion

In conclusion, the author has shown that nanocomposite materials universally show a similar power law decay in electromechanical signal due to the Mullin's effect and which was described using a modified model based on Basquin's law of fatigue. By fitting this model to literary datasets, nanocomposites were found to on average scale as $C^{-0.1}$, which was supported by theory and literary data. Furthermore, through this model a way in which the required number of conditioning cycles to reach a steady state signal was demonstrated, with predicted values closely matching reported experimental ones. This work presents methods in which researchers can better gauge a nanocomposite strain sensor's potential for application and allows for the processing of signal outputs to better facilitate reaching the long term of goal of applying these materials as health monitors.

Methods

Data from literary sources was extracted and fitted using the "Digitizer" function in Origin 2019 software. Literary datasets were chosen from reports on resistive strain sensors, which used conductive polymer-based nanocomposites as the sensing material, and reported cyclic data that could be extrapolated. As calculated values are extrapolated from published and not raw data, all values are to be taken as an estimate. All values for extrapolated data can be found in the Supplementary Information.

The author declares no competing financial interest.

Supporting Information

Supporting Information includes extrapolated values and fitted data from literary sources (Fig S1-S9 and Tables S1-S3. This Supporting Information is available online free of charge.

Acknowledgements

This work was supported by strategic development funding from the University of Sussex.

References

1. Perera, C., *Sensing as a Service for Internet of Things: A Roadmap*, **2018**, Leanpub, Victoria, Canada.
2. *2019 Annual Report, Graphene Flagship*
3. Boland, C. S. Stumbling through the Research Wilderness, Standard Methods to Shine Light on Electrically Conductive Nanocomposites for Future Healthcare Monitoring. *ACS Nano*, **2019**, *13*, 13627-13636
4. Ramalingame, R., Bouhamed, A., Rajendran, D., da Veiga Torres, R., Hu, Z. and Kanoun, O., *Highly Sensitive Polymer/Multiwalled Carbon Nanotubes Based Pressure and Strain Sensors for Robotic Applications*, in *New Trends in Robot Control*. **2020**, 371-382.
5. Choi, D. Y., Kim, M. H., Oh, Y. S., Jung, S. H., Jung, J. H., Sung, H. J., Lee, H. W. and Lee, H. M. Highly Stretchable, Hysteresis-Free Ionic Liquid-Based Strain Sensor for Precise Human Motion Monitoring. *ACS Appl. Mater. Interfaces*, **2017**, *9*, 1770-1780
6. Ku-Herrera, J. J. and Aviles, F. Cyclic Tension and Compression Piezoresistivity of Carbon Nanotube/Vinyl Ester Composites in the Elastic and Plastic Regimes. *Carbon*, **2012**, *50*, 2592-2598
7. Meng, Q., Kenelak, V., Chand, A., Kang, H., Han, S. and Liu, T. A Highly Flexible, Electrically Conductive, and Mechanically Robust Graphene/Epoxy Composite Film for Its Self-Damage Detection. *J. Appl. Polym. Sci.*, **2020**, 48991
8. Lee, S., Shin, S., Lee, S., Seo, J., Lee, J., Son, S., Cho, H. J., Algadi, H., Al-Sayari, S., Kim, D. E. and Lee, T. Ag Nanowire Reinforced Highly Stretchable Conductive Fibers for Wearable Electronics. *Adv. Funct. Mater.*, **2015**, *25*, 3114-3121
9. Luo, C., Tian, B., Liu, Q., Feng, Y. and Wu, W. One-Step-Printed, Highly Sensitive, Textile-Based, Tunable Performance Strain Sensors for Human Motion Detection. *Adv. Mat. Tech.*, **2020**, *5*, 1900925
10. He, T., Lin, C., Shi, L., Wang, R. and Sun, J. Through-Layer Buckle Wavelength-Gradient Design for the Coupling of High Sensitivity and Stretchability in a Single Strain Sensor. *ACS Appl. Mater. Interfaces*, **2018**, *10*, 9653-9662
11. Li, Y. Q., Huang, P., Zhu, W. B., Fu, S. Y., Hu, N. and Liao, K. Flexible Wire-Shaped Strain Sensor from Cotton Thread for Human Health and Motion Detection. *Sci. Rep.*, **2017**, *7*, 45013
12. Wang, Y. L., Jia, Y. Y., Zhou, Y. J., Wang, Y., Zheng, G. Q., Dai, K., Liu, C. T. and Shen, C. Y. Ultra-Stretchable, Sensitive and Durable Strain Sensors Based on Polydopamine Encapsulated Carbon Nanotubes/Elastic Bands. *J. Mater. Chem. C*, **2018**, *6*, 8160-8170
13. Huang, W. P., Li, J. H., Zhao, S. F., Han, F., Zhang, G. P., Sun, R. and Wong, C. P. Highly Electrically Conductive and Stretchable Copper Nanowires-Based Composite for Flexible and Printable Electronics. *Compos. Sci. Technol.*, **2017**, *146*, 169-176
14. Gao, L., Thostenson, E. T., Zhang, Z. and Chou, T.-W. Sensing of Damage Mechanisms in Fiber-Reinforced Composites under Cyclic Loading Using Carbon Nanotubes. *Adv. Funct. Mat.*, **2009**, *19*, 123-130
15. Wu, S. Y., Peng, S. H. and Wang, C. H. Stretchable Strain Sensors Based on Pdms Composites with Cellulose Sponges Containing One- and Two-Dimensional Nanocarbons. *Sens. Actuators A*, **2018**, *279*, 90-100
16. Gonzalez-Dominguez, J. M., Martin, C., Dura, O. J., Merino, S. and Vazquez, E. Smart Hybrid Graphene Hydrogels: A Study of the Different Responses to Mechanical Stretching Stimulus. *ACS Appl. Mater. Interfaces*, **2018**, *10*, 1987-1995
17. Wu, S., Peng, S. and Wang, C. H. Stretchable Strain Sensors Based on Pdms Composites with Cellulose Sponges Containing One- and Two-Dimensional Nanocarbons. *Sens. Actuators A*, **2018**, *279*, 90-100
18. Pegan, J. D., Zhang, J., Chu, M., Nguyen, T., Park, S.-J., Paul, A., Kim, J., Bachman, M. and Khine, M. Skin-Mountable Stretch Sensor for Wearable Health Monitoring. *Nanoscale*, **2016**, *8*, 17295-17303
19. Boland, C. S., Khan, U., Backes, C., O'Neill, A., McCauley, J., Duane, S., Shanker, R., Liu, Y., Jurewicz, I., Dalton, A. B. and Coleman, J. N. Sensitive, High-Strain, High-Rate Bodily Motion Sensors Based on Graphene-Rubber Composites. *ACS Nano*, **2014**, *8*, 8819-8830

20. Zhang, H., Han, W., Xu, K., Zhang, Y., Lu, Y., Nie, Z., Du, Y., Zhu, J. and Huang, W. Metallic Sandwiched-Aerogel Hybrids Enabling Flexible and Stretchable Intelligent Sensor. *Nano Lett.*, **2020**, *20*, 3449–3458
21. Pei, Z., Zhang, Q., Liu, Y., Zhao, Y., Dong, X., Zhang, Y., Zhang, W. and Sang, S. A High Gauge-Factor Wearable Strain Sensor Array Via 3d Printed Mold Fabrication and Size Optimize of Silver Coated Carbon Nanotubes. *Nanotechnology*, **2020**, *31*, 305501
22. Yang, H., Yao, X. F., Zheng, Z., Gong, L. H., Yuan, L., Yuan, Y. A. and Liu, Y. H. Highly Sensitive and Stretchable Graphene-Silicone Rubber Composites for Strain Sensing. *Compos. Sci. Technol.*, **2018**, *167*, 371-378
23. Natarajan, T. S., Eshwaran, S. B., Stockelhuber, K. W., Wiessner, S., Potschke, P., Heinrich, G. and Das, A. Strong Strain Sensing Performance of Natural Rubber Nanocomposites. *ACS Appl. Mater. Interfaces*, **2017**, *9*, 4860-4872
24. Goncalves, B. F., Oliveira, J., Costa, P., Correia, V., Martins, P., Botelho, G. and Lanceros-Mendez, S. Development of Water-Based Printable Piezoresistive Sensors for Large Strain Applications. *Composites Part B*, **2017**, *112*, 344-352
25. Zhou, Y., Zhan, P., Ren, M., Zheng, G., Dai, K., Mi, L., Liu, C. and Shen, C. Significant Stretchability Enhancement of a Crack-Based Strain Sensor Combined with High Sensitivity and Superior Durability for Motion Monitoring. *ACS Appl. Mater. Interfaces*, **2019**, *11*, 7405-7414
26. Ding, Y. C., Yang, J., Tolle, C. R. and Zhu, Z. T. A Highly Stretchable Strain Sensor Based on Electrospun Carbon Nanofibers for Human Motion Monitoring. *RSC Adv.* **2016**, *6*, 79114-79120
27. Zhang, Y., He, P., Luo, M., Xu, X., Dai, G. and Yang, J. Highly Stretchable Polymer/Silver Nanowires Composite Sensor for Human Health Monitoring. *Nano Res.*, **2020**, 1-8
28. Wang, S., Xiao, P., Liang, Y., Zhang, J. W., Huang, Y. J., Wu, S., Kuo, S. W. and Chen, T. Network Cracks-Based Wearable Strain Sensors for Subtle and Large Strain Detection of Human Motions. *J. Mater. Chem. C*, **2018**, *6*, 5140-5147
29. Wu, S., Zhang, J., Ladani, R. B., Ravindran, A. R., Mouritz, A. P., Kinloch, A. J. and Wang, C. H. Novel Electrically Conductive Porous Pdms/Carbon Nanofiber Composites for Deformable Strain Sensors and Conductors. *ACS Appl. Mater. Interfaces*, **2017**, *9*, 14207-14215
30. Lin, L., Liu, S., Zhang, Q., Li, X., Ji, M., Deng, H. and Fu, Q. Towards Tunable Sensitivity of Electrical Property to Strain for Conductive Polymer Composites Based on Thermoplastic Elastomer. *ACS Appl. Mater. Interfaces*, **2013**, *5*, 5815-5824
31. Wang, X., Meng, S., Tebyetekerwa, M., Li, Y., Pionteck, J., Sun, B., Qin, Z. and Zhu, M. Highly Sensitive and Stretchable Piezoresistive Strain Sensor Based on Conductive Poly(Styrene-Butadiene-Styrene)/Few Layer Graphene Composite Fiber. *Composites Part A*, **2018**, *105*, 291-299
32. Bauman, J. T., *Fatigue, Stress, and Strain of Rubber Components* Hanser Publications, Cincinnati, OH, **2008**.
33. *Msc.Marc Volume A: Theory and User Information, Version 2001*. 2001; Available from: http://www.mate.tue.nl/~piet/inf/mrc/pdf/vola2001.pdf.
34. Cantournet, S., Desmorat, R. and Besson, J. Mullins Effect and Cyclic Stress Softening of Filled Elastomers by Internal Sliding and Friction Thermodynamics Model. *Int. J. Solids Struct.*, **2009**, *46*, 2255-2264
35. Yu, S. L., Wang, X. P., Xiang, H. X., Zhu, L. P., Tebyetekerwa, M. and Zhu, M. F. Superior Piezoresistive Strain Sensing Behaviors of Carbon Nanotubes in One-Dimensional Polymer Fiber Structure. *Carbon*, **2018**, *140*, 1-9
36. Diani, J., Fayolle, B. and Gilormini, P. A Review on the Mullins Effect. *Eur. Polym. J.*, **2009**, *45*, 601-612
37. Kraus, G., *Mechanical Losses in Carbon-Black-Filled Rubbers* J. Appl. Polym. Sci. Symp., **1984.**
38. Merabia, S., Sotta, P. and Long, D. R. Unique Plastic and Recovery Behavior of Nanofilled Elastomers and Thermoplastic Elastomers (Payne and Mullins Effects). *J. Polym. Sci. Part B: Polym. Phys*, **2010**, *48*, 1495-1508

39. Semkiv, M., Anderson, P. D. and Hütter, M. Two-Scale Model for the Effect of Physical Aging in Elastomers Filled with Hard Nanoparticles. *J. Comput. Phys.*, **2017**, *350*, 184-206
40. Merabia, S., Sotta, P. and Long, D. R. A Microscopic Model for the Reinforcement and the Nonlinear Behavior of Filled Elastomers and Thermoplastic Elastomers (Payne and Mullins Effects). *Macromolecules*, **2008**, *41*, 8252-8266
41. Ponnamma, D., Kumar Sadasivuni, K., Strankowski, M., Moldenaers, P., Thomas, S. and Grohens, Y. Interrelated Shape Memory and Payne Effect in Polyurethane/Graphene Oxide Nanocomposites. *RSC Adv.*, **2013**, *3*, 16068-16079
42. Xing, W., Tang, M., Wu, J., Huang, G., Li, H., Lei, Z., Fu, X. and Li, H. Multifunctional Properties of Graphene/Rubber Nanocomposites Fabricated by a Modified Latex Compounding Method. *Compos. Sci. Technol.* **2014**, *99*, 67-74
43. Sahimi, M. Applications of Percolation Theory, **1994,** *CRC Press*.
44. Stauffer, D. and Aharony, A., *Introduction to Percolation Theory*, **1994**, CRC Press.
45. Stankovich, S., Dikin, D. A., Dommett, G. H. B., Kohlhaas, K. M., Zimney, E. J., Stach, E. A., Piner, R. D., Nguyen, S. T. and Ruoff, R. S. Graphene-Based Composite Materials. *Nature*, **2006**, *442*, 282-286
46. Gagel, A., Lange, D. and Schulte, K. On the Relation between Crack Densities, Stiffness Degradation, and Surface Temperature Distribution of Tensile Fatigue Loaded Glass-Fibre Non-Crimp-Fabric Reinforced Epoxy. *Composites Part A*, **2006**, *37*, 222-228
47. Böger, L., Wichmann, M. H. G., Meyer, L. O. and Schulte, K. Load and Health Monitoring in Glass Fibre Reinforced Composites with an Electrically Conductive Nanocomposite Epoxy Matrix. *Compos. Sci. Technol.*, **2008**, *68*, 1886-1894
48. D'Antuono, P. An Analytical Relation between the Weibull and Basquin Laws for Smooth and Notched Specimens and Application to Constant Amplitude Fatigue. *Fatigue Fract. Eng. Mater. Struct.*, **2020**, *43*, 991-1004
49. Kun, F., Carmona, H. A., Andrade, J. S. and Herrmann, H. J. Universality Behind Basquin's Law of Fatigue. *Phys. Rev. Lett.*, **2008**, *100*, 094301
50. American Society for Testing, M., *Manual on Low Cycle Fatigue Testing*, **1969**, ASTM International, Philadelphia, Pa.
51. Hearn, E. J., *Chapter 11 - Fatigue, Creep and Fracture*, in *Mechanics of Materials 2*, **1997**, Butterworth-Heinemann: Oxford. 443-508.
52. Wang, G.-T., Liu, H.-Y., Saintier, N. and Mai, Y.-W. Cyclic Fatigue of Polymer Nanocomposites. *Eng. Failure Anal.*, **2009**, *16*, 2635-2645
53. Kim, T. K., Kim, J. K. and Jeong, O. C. Measurement of Nonlinear Mechanical Properties of Pdms Elastomer. *Microelectron. Eng.*, **2011**, *88*, 1982-1985
54. Shokrieh, M. M., Esmkhani, M., Haghighatkhah, A. R. and Zhao, Z. Flexural Fatigue Behavior of Synthesized Graphene/Carbon-Nanofiber/Epoxy Hybrid Nanocomposites. *Mater. Des. (1980-2015)*, **2014**, *62*, 401-408
55. Wan, S. and Cheng, Q. Fatigue-Resistant Bioinspired Graphene-Based Nanocomposites. *Adv. Funct. Mater.*, **2017**, *27*, 1703459
56. Zhou, Y., Rangari, V., Mahfuz, H., Jeelani, S. and Mallick, P. K. Experimental Study on Thermal and Mechanical Behavior of Polypropylene, Talc/Polypropylene and Polypropylene/Clay Nanocomposites. *Mater. Sci. Eng. A*, **2005**, *402*, 109-117
57. do Lee, C. Effect of Strain Rate on Elastic-Plastic Deformation in High Cycle Fatigue Properties. *Met. Mater. Int.*, **2014**, *20*, 1027-1035
58. Wang, Y., Jia, Y., Zhou, Y., Wang, Y., Zheng, G., Dai, K., Liu, C. and Shen, C. Ultra-Stretchable, Sensitive and Durable Strain Sensors Based on Polydopamine Encapsulated Carbon Nanotubes/Elastic Bands. *J. Mater. Chem. C*, **2018**, *6*, 8160-8170
59. Yang, H., Yao, X., Zheng, Z., Gong, L., Yuan, L., Yuan, Y. and Liu, Y. Highly Sensitive and Stretchable Graphene-Silicone Rubber Composites for Strain Sensing. *Compos. Sci. Technol.*, **2018**, *167*, 371-378
60. Lee, H., Kim, M. J., Kim, J. H., Lee, J.-Y., Ji, E., Capasso, A., Choi, H.-J., Shim, W. and Lee, G.-H. Highly Flexible Graphene Nanoplatelet-Polydimethylsiloxane Strain Sensors with Proximity-Sensing Capability. *Mater. Res. Express*, **2020**, *7*, 045603

61. Fleck, N. A., Kang, K. J. and Ashby, M. F. Overview No. 112: The Cyclic Properties of Engineering Materials. *Acta Metall. Mater.*, **1994**, *42*, 365-381
62. Lake, G. J. and Lindley, P. B. The Mechanical Fatigue Limit for Rubber. *J. Appl. Polym. Sci.*, **1965**, *9*, 1233-1251
63. Wang, X., Qiu, Y., Cao, W. and Hu, P. Highly Stretchable and Conductive Core–Sheath Chemical Vapor Deposition Graphene Fibers and Their Applications in Safe Strain Sensors. *Chem. Mater.*, **2015**, *27*, 6969-6975
64. Wu, Q., Zou, S., Gosselin, F. P., Therriault, D. and Heuzey, M.-C. 3d Printing of a Self-Healing Nanocomposite for Stretchable Sensors. *J. Mater. Chem. C*, **2018**, *6*, 12180-12186
65. Lu, L., Zhou, Y., Pan, J., Chen, T., Hu, Y., Zheng, G., Dai, K., Liu, C., Shen, C., Sun, X. and Peng, H. Design of Helically Double-Leveled Gaps for Stretchable Fiber Strain Sensor with Ultralow Detection Limit, Broad Sensing Range, and High Repeatability. *ACS Appl. Mater. Interfaces*, **2019**, *11*, 4345-4352
66. Gao, Y., Guo, F., Cao, P., Liu, J., Li, D., Wu, J., Wang, N., Su, Y. and Zhao, Y. Winding-Locked Carbon Nanotubes/Polymer Nanofibers Helical Yarn for Ultrastretchable Conductor and Strain Sensor. *ACS Nano*, **2020**, *14*, 3442-3450
67. Liu, Q., Chen, J., Li, Y. and Shi, G. High-Performance Strain Sensors with Fish-Scale-Like Graphene-Sensing Layers for Full-Range Detection of Human Motions. *ACS Nano*, **2016**, *10*, 7901-7906
68. Jeong, Y. R., Kim, J., Xie, Z., Xue, Y., Won, S. M., Lee, G., Jin, S. W., Hong, S. Y., Feng, X., Huang, Y., Rogers, J. A. and Ha, J. S. A Skin-Attachable, Stretchable Integrated System Based on Liquid Gainsn for Wireless Human Motion Monitoring with Multi-Site Sensing Capabilities. *NPG Asia Mater.*, **2017**, *9*, e443-e443
69. Lee, W. S., Kim, D., Park, B., Joh, H., Woo, H. K., Hong, Y.-K., Kim, T.-i., Ha, D.-H. and Oh, S. J. Multiaxial and Transparent Strain Sensors Based on Synergetically Reinforced and Orthogonally Cracked Hetero-Nanocrystal Solids. *Adv. Funct. Mater.*, **2019**, *29*, 1806714
70. Min, S.-H., Lee, G.-Y. and Ahn, S.-H. Direct Printing of Highly Sensitive, Stretchable, and Durable Strain Sensor Based on Silver Nanoparticles/Multi-Walled Carbon Nanotubes Composites. *Composites Part B*, **2019**, *161*, 395-401

Figures:

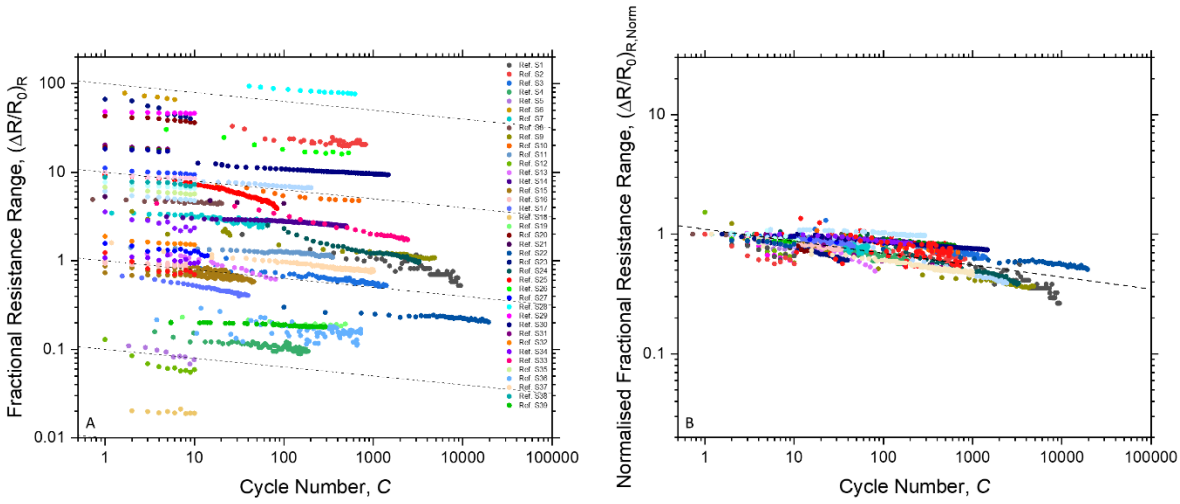

Figure 1. Fractional resistance change range, $(\Delta R/R_0)_R$, as a function of cycle number. (A) Curves from 54 datasets show similar power law scaling as denoted by dashed lines representing $(\Delta R/R_0)_R \propto C^{-0.1}$. (B) Normalised fractional resistance change range, $(\Delta R/R_0)_{R,Norm}$, as a function of cycle number shows that all datasets sit on master curve that scales as $\sim C^{-0.1}$.

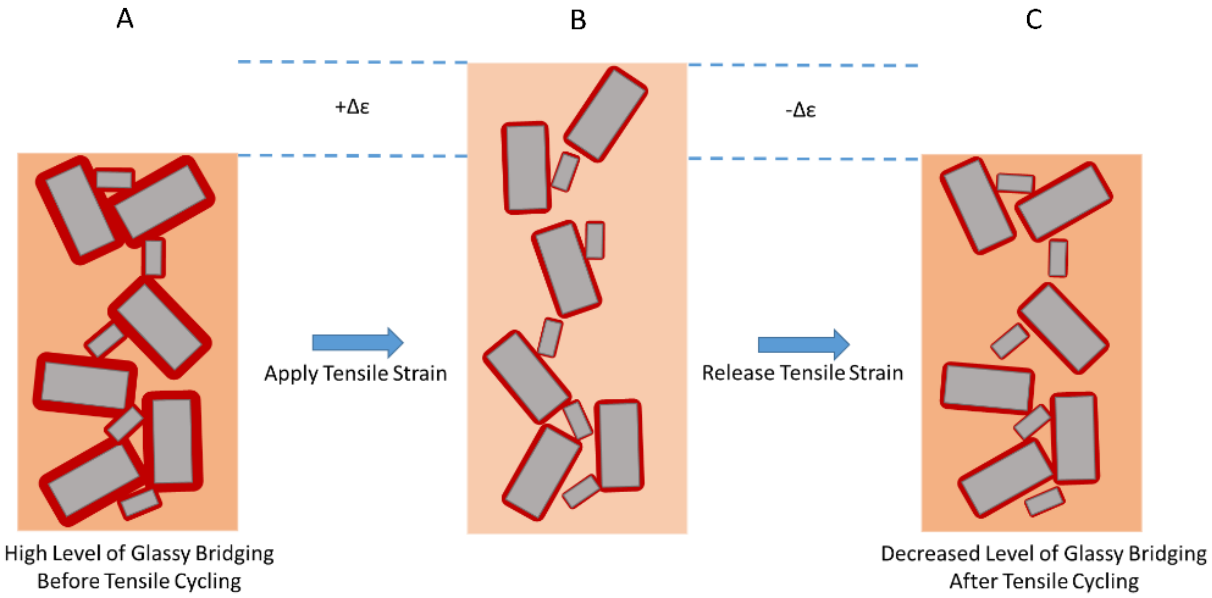

Figure 1. Atypical polymer-based nanocomposite under cyclic loading. (A) Before cycling, nanofillers, depicted here as two-dimensional nanosheets (grey rectangles), are coated in a glassy layer (red regions) and have formed an interconnected network of fillers through adjoining layers, known as glassy bridges. (B) During loading, fluidisation of the glassy microstructure occurs, causing the regions to trend towards a more amorphous structure. (C) After loading release, the density of the glassy microstructure has decreased, leaving the nanofiller network less connected to the matrix (orange region) and to nearest neighbours resulting in diminished responsivity of the network to subsequent loading cycles.

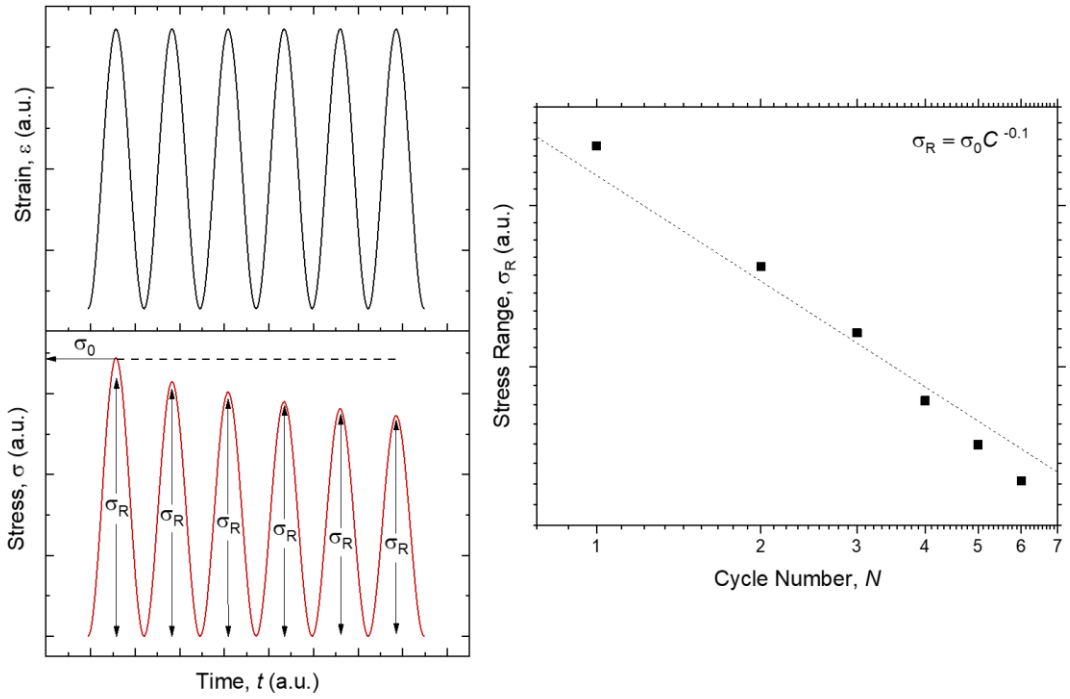

Figure 2. Basquin scaling in hypothetical cyclic mechanical data. (A-B) Data presented shows that with a constant strain loading there is an observed decrease in stress range (σ_R) with respect to the initial stress range (σ_0) as cycle number (C) increases. (C) Wöhler's plot presenting σ_R as a function of C where the dashed line represents a fitting of Eq. 1.

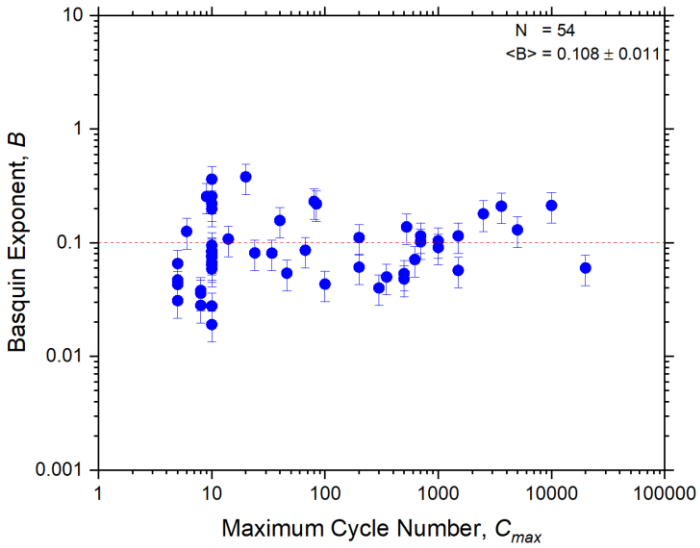

Figure 3. Basquin exponent from nanocomposite strain sensor literature. The Basquin exponent (B) derived from fitting the data sets from Fig 1A in SI Fig S1-S7 were plotted as a function of maximum cycle number (C_{max}). Values for the exponent were found to vary between ~0.02 and ~0.4, with a mean of 0.108 ± 0.011 from 54 data sets reported.

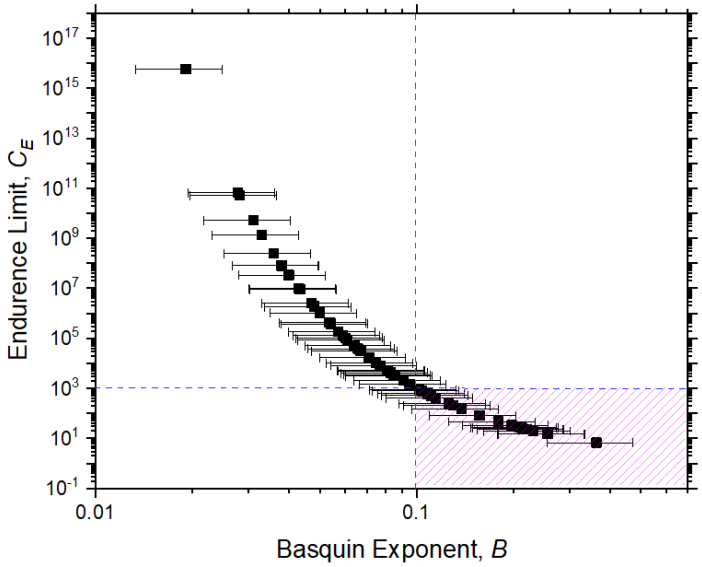

Figure 4. Conditioning requirements to reach steady state signal. A plot of the calculated values of endurance limit, C_E, from Eq. 11 verse the Basquin Exponents from literary data sets in Fig. 4 calculated using Eq. 7 (see SI Table S1). An optimum processability region was designated as nanocomposites having a Basquin exponent at or above the theoretically expected value of 0.1, which from this plot presents the lowest values of condition cycles to reach C_E.

ToC:

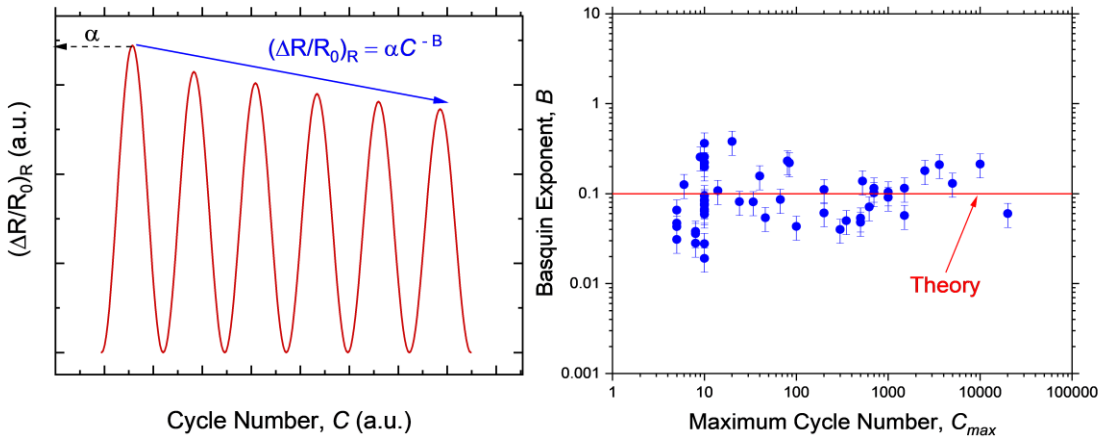
α
$(\Delta R/R_0)_R = \alpha C^{-B}$
$(\Delta R/R_0)_R$ (a.u.)
Cycle Number, C (a.u.)
Basquin Exponent, B
Theory
Maximum Cycle Number, C_{max}
10
1
0.1
0.01
0.001
1
10
100
1000
10000
100000